BIOCHEMISTRY
including biophysical chemistry & molecular biology

Article

pubs.acs.org/biochemistry

Biochemical and Structural Analysis of an Eis Family Aminoglycoside Acetyltransferase from *Bacillus anthracis*

Keith D. Green,[⊥,◆] Tapan Biswas,[†,◆] Changsoo Chang,[▽] Ruiying Wu,[▽] Wenjing Chen,[‡,§] Brian K. Janes,[∥] Dominika Chalupska,[○] Piotr Gornicki,[○] Philip C. Hanna,[∥] Oleg V. Tsodikov,[⊥] Andrzej Joachimiak,[#,▽] and Sylvie Garneau-Tsodikova*[,⊥]

[†]Department of Medicinal Chemistry, [‡]Life Sciences Institute, [§]Chemical Biology Doctoral Program, and [∥]Department of Microbiology and Immunology, University of Michigan, Ann Arbor, Michigan 48109-2216, United States

[⊥]Department of Pharmaceutical Sciences, University of Kentucky, Lexington, Kentucky 40536-0596, United States

[#]Department of Biochemistry and Molecular Biology and [○]Department of Molecular Genetics and Cell Biology, University of Chicago, Chicago, Illinois 60637, United States

[▽]Structural Biology Center, Biosciences, Argonne National Laboratory, Argonne, Illinois 60439, United States

Supporting Information

ABSTRACT: Proteins from the enhanced intracellular survival (Eis) family are versatile acetyltransferases that acetylate amines at multiple positions of several aminoglycosides (AGs). Their upregulation confers drug resistance. Homologues of Eis are present in diverse bacteria, including many pathogens. Eis from *Mycobacterium tuberculosis* (Eis_*Mtb*) has been well characterized. In this study, we explored the AG specificity and catalytic efficiency of the Eis family protein from *Bacillus anthracis* (Eis_*Ban*). Kinetic analysis of specificity and catalytic efficiency of acetylation of six AGs indicates that Eis_*Ban* displays significant differences from Eis_*Mtb* in both substrate binding and catalytic efficiency. The number of acetylated amines was also different for several AGs, indicating a distinct regiospecificity of Eis_*Ban*. Furthermore, most recently identified inhibitors of Eis_*Mtb* did not inhibit Eis_*Ban*, underscoring the differences between these two enzymes. To explain these differences, we determined an Eis_*Ban* crystal structure. The comparison of the crystal structures of Eis_*Ban* and Eis_*Mtb* demonstrates that critical residues lining their respective substrate binding pockets differ substantially, explaining their distinct specificities. Our results suggest that acetyltransferases of the Eis family evolved divergently to garner distinct specificities while conserving catalytic efficiency, possibly to counter distinct chemical challenges. The unique specificity features of these enzymes can be utilized as tools for developing AGs with novel modifications and help guide specific AG treatments to avoid Eis-mediated resistance.

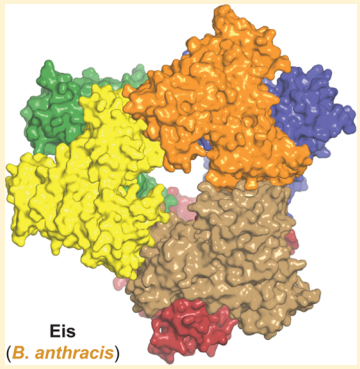

Bacillus anthracis (*Ban*), a Gram-positive bacterium, is the cause of the deadly infectious disease anthrax. The *Bacillus* genus includes other pathogens such as *Bacillus cereus*[1] and *Bacillus thuringiensis*, although these are less infectious. *B. anthracis* resides in soil and typically infects plant-eating mammals. Infection of carnivores and humans occurs usually through direct contact with highly resilient endospores. Upon infection, endospores germinate into active bacilli and multiply. The combined release of three proteins from these bacilli (lethal factor, edema factor, and protective antigen), which interact with their specific targets at the mammalian cell surface, leads to severe toxemia, known as anthrax disease (cutaneous and gastrointestinal forms). When acquired through inhalation of *B. anthracis* spores (pulmonary form), anthrax initially causes flu-like symptoms, but eventually leads to a fatal respiratory collapse.[2] This acute pulmonary infectious ability underlies potential use of *B. anthracis* as a bioweapon. Deliberate dissemination of an aerosolized form of virulent strains of *B. anthracis* (such as the Ames, Vollum, and other potential man-made derivatives) as a bioweapon is a real threat to both humans and livestock. Vaccines based on spores from the attenuated Sterne strain of *B. anthracis* are effective against anthrax, but vaccination of a majority of the human population is a difficult task,[3,4] and presently available vaccines are not entirely safe.[5,6] Therefore, antibiotics are needed for prophylactic treatment prior to potential exposure as well as postexposure emergency treatment of inhalation anthrax.[7] Existing drugs (large doses of intravenous and oral antibiotics, e.g., ciprofloxacin, doxycycline, erythromycin, vancomycin, or penicillin) are only effective if started in the early stages of infection. In addition, some *B. anthracis* strains have already developed resistance to some of the aforementioned antibiotics.[8−11] For effective treatment of inhalation anthrax in humans and infected animals, new antibiotics are needed.

Received: March 6, 2015
Revised: April 9, 2015
Published: April 30, 2015

DOI: 10.1021/acs.biochem.5b00244
Biochemistry 2015, 54, 3197−3206

Biochemical and structural studies are underway to develop new drugs against *B. anthracis* and explore new drug targets in order to inhibit spore germination,[12] DNA replication, and the vegetative growth,[13−18] disable the released toxins and other virulence factors,[19−22] and utilize aminoglycosides (AGs) as toxin inhibitors and potential anti-anthrax drugs.[20,23−25] In this study, we investigated a highly potent AG acetylator encoded by gene *bas2743* of *B. anthracis* (Eis_*Ban*). Eis proteins from *Mycobacterium tuberculosis* (Eis_*Mtb*), *Mycobacterium smegmatis* (Eis_*Msm*), and *Anabaena variabilis* (Eis_*Ava*) catalyze the transfer of an acetyl group to the amino group(s) of various AGs[26−28] and amino acid residues in lysine-containing drugs and proteins.[29,30] When upregulated, Eis_*Mtb* is known to cause resistance to the AG kanamycin A (KAN) in tuberculosis patients.[31] Similarly, upregulation of Eis in *B. anthracis* may lead to resistance to AG antibiotics. To address the acetylation potential and possible differences in substrate specificity between Eis_*Ban* and Eis_*Mtb*, and Eis from other organisms, we carried out a combined structural and functional investigation of Eis_*Ban*. Our study revealed a highly divergent AG binding site endowing a remarkably distinct substrate specificity and highly potent AG acetylating activity.

MATERIALS AND METHODS

Bacterial Strains, Plasmids, Materials, and Instrumentation. The chemically competent *Escherichia coli* TOP10 and BL21 (DE3) strains were purchased from Invitrogen (Carlsbad, CA). All restriction enzymes, T4 DNA ligase, and Phusion DNA polymerase were purchased from NEB (Ipswich, MA). PCR primers were purchased from Integrated DNA Technologies (IDT; Coralville, IA). The pET15b vector was purchased from Novagen (Gibbstown, NJ). DNA sequencing was performed at the University of Michigan DNA Sequencing Core. All reagents were used as received without further purification. DTNB, AcCoA, AGs (apramycin (APR), amikacin (AMK), gentamicin (GEN), hygromycin (HYG), KAN, neomycin B (NEO), sisomicin (SIS), spectinomycin (SPT), streptomycin (STR), and ribostamycin (RIB)) (Figure S1, Supporting Information), ampicillin, chloramphenicol, ciprofloxacin, erythromycin, isoniazid, norfloxacin, and chlorhexidine (**1**) were purchased from Sigma-Aldrich (Milwaukee, WI). The AG geneticin (G418) was purchased from Research Products International (Mt Prospect, IL). The rest of the AGs (neamine (NEA), netilmicin (NET), paromomycin (PAR), and tobramycin (TOB)) (Figure S1) were purchased from AK Scientific (Mountain View, CA). The spectrophotometric assays were performed on a multimode SpectraMax M5 plate reader using 96-well plates (Fisher Scientific; Pittsburgh, PA). Silica gel 60 F_{254} plates (Merck) were used for thin-layer chromatography (TLC) analysis. Liquid chromatography mass spectrometry (LCMS) was performed on a Shimadzu LCMS-2019EV equipped with a SPD-20AV UV−vis detector and a LC-20AD liquid chromatograph.

Cloning, Overproduction, and Purification of Selenomethionine-Substituted Eis_*Ban* for Structural Studies. The Eis_*Ban* acetyltransferase (GI: 753454082) coding sequence cassette was amplified by PCR from chromosomal DNA of *B. anthracis* Sterne strain using primers compatible with the ligation-independent cloning vector pMCSG7 and cloned into pMCSG7 using the ligation-independent protocol.[32] The recombinant Eis_*Ban* with an N-terminal His_6-tag and a TEV protease recognition site (ENLYFQ↓S) was expressed in an *E. coli* BL21 (DE3) strain harboring a pMAGIC plasmid encoding one rare *E. coli* tRNAs for Arg codons AGG/AGA. Expression of the His_6-tagged fusion protein in *E. coli* BL21 (DE3) strain carrying the pMAGIC vector was induced with isopropyl β-D-thiogalactoside (IPTG). A selenomethionine (SeMet) derivative of the expressed protein was prepared and purified using Ni-affinity chromatography as described previously.[33,34] Briefly, the harvested cells, containing SeMet-labeled protein, were resuspended in lysis buffer (500 mM NaCl, 5% [v/v] glycerol, 50 mM HEPES pH 8.0, 10 mM imidazole, and 10 mM β-mercaptoethanol), and the lysate was clarified by centrifugation, filtered through a 0.44 μm membrane, and applied to a 5 mL HiTrap Ni-NTA column (GE Health Systems) on an AKTAxpress system. The eluted His_6-tagged protein was further purified by size exclusion chromatography (Hiload 26/600 Superdex 200 pg GE) with crystallization buffer containing 100 mM NaCl, 20 mM HEPES pH 8.0, and 2 mM dithiothreitol (DTT) and then concentrated to 30 mg/mL for crystallization using an Amicon Ultra centrifugal filter device with a 10 000-MW cutoff (Millipore), flash-frozen, and stored in liquid nitrogen.

Overproduction and Purification of Eis Proteins for Biochemical Studies. The Eis_*Mtb*,[27] Eis_*Msm*,[28] and Eis_*Ava*[26] proteins (with a N-terminal His_6-tag) were prepared as previously reported. Eis_*Ban* was overexpressed and purified using the exact procedure used for Eis_*Mtb*[27] and stored at 4 °C in 50 mM Tris pH 8.0. After purification, 3.2 mg of the 48 213-Da Eis_*Ban* ($NHis_6$-tagged) protein was obtained per liter of culture (Figure S2, Supporting Information).

Determination of the AG Selectivity Profile of Eis_*Ban* by a Spectrophotometric Assay. The substrate specificity and acetlytransferase activity of Eis_*Ban* were determined using the Ellman method as previously reported.[27] The free thiol of CoA generated as a byproduct of the acetylation reaction reacts with the DTNB indicator releasing 2-nitro-5-thiobenzene, which absorbs at 412 nm (ε_{412} = 14 150 M^{-1} cm^{-1}). Reactions (200 μL) containing Tris (50 mM pH 8.0), AG (100 μM), AcCoA (500 μM), and DTNB (2 mM) were initiated by addition of Eis_*Ban* (0.5 μM final concentration) and were monitored every 30 s for 30 min at 25 °C.

Determination and Confirmation of Number of Acetylation Sites by the Spectrophotometric Assay and Mass Spectrometry. The number of times Eis_*Ban* acetylated each AG was determined though the use of two reactions per each AG. The first reaction contained 1 equiv of AcCoA for every equivalent of AG, and the second contained 5 equiv of AcCoA for 1 equiv of AG. Briefly, reaction mixtures (200 μL) containing AcCoA (100 μM, 1 equiv or 500 μM, 5 equiv), AG (100 μM), Tris (50 mM, pH 8.0), and DTNB (2 mM) were initiated by the addition of Eis_*Ban* (0.5 μM). Reaction progress at 25 °C was monitored at 412 nm as above until a plateau was achieved. Representative plots are presented in Figure S3, Supporting Information, and all data are summarized in Table 1. To confirm the findings of the UV−vis assay, a final reaction (20 μL) containing AcCoA (3.35 mM, 5 equiv), AG (0.67 mM, 1 equiv), Tris (50 mM, pH 8.0), and Eis_*Ban* (10 μM) was carried out at 25 °C. Reaction were quenched by precipitating the enzyme with an equal volume of ice-cooled MeOH. After 20 min at −20 °C, the precipitate was removed by centrifugation (13 000 rpm, room temperature, 10 min). The masses of the AG species in the supernatant in each sample were determined by LCMS in positive mode, after a 1:3 dilution in H_2O, by using H_2O with 0.1% formic acid as the eluent for the LC. Mass spectra are provided in Figure S4, Supporting Information and summarized in Table S1, Supporting Information.

DOI: 10.1021/acs.biochem.5b00244
Biochemistry 2015, 54, 3197−3206

Table 1. Comparison of Levels of Acetylation of AGs by Eis from *A. variabilis*, *B. anthracis*, *M. smegmatis*, and *M. tuberculosis*

AG	*B. anthracis*	*A. variabilis*[a]	*M. smegmatis*[b]	*M. tuberculosis*[c]
AMK	di	tri	tri	tri
APR	di	mono	di	×[d]
HYG	di	mono	mono	di
KAN	di	tri	di	di
NEA	tri	tri	tri	tri
NEO	tri	tri	tri	tri
NET	mono	di	di	di
PAR	tri	tri	tri	di
RIB	tri	tri	tri	tri
SIS	di	di	tri	tri
SPT	×	×	×	×
STR	×	×	×	×
TOB	×	–[e]	tetra	tetra

[a]These data were previously reported.[26] [b]These data were previously reported.[28] [c]These data were previously reported.[27] [d]×, indicates that the AG is not a substrate of the enzyme. [e]–, not reported.

Kinetic Characterization of Eis_*Ban* Activity. Michaelis–Menten kinetic parameters (K_m and k_{cat}) were determined for several AGs (AMK, APR, KAN, NEO, and SIS) and AcCoA with the Eis_*Ban* purified enzyme. To determine the kinetic parameters of the AGs, the concentration of AcCoA (500 μM) was held constant. To determine the AcCoA kinetic parameters, the concentration of KAN (500 μM) was held constant. In short, solutions containing AG (0–200 μM for KAN and PAR, or 0–2000 μM for AMK and NEO final concentrations) were used to initiate a premixed solution of AcCoA (500 μM), Eis_*Ban* (0.25 μM), DTNB (2 mM), and Tris (50 mM, pH 8.0). Reactions were set up independently and monitored as above, taking measurements every 15–20 s for 30 min, in the linear range of product accumulation over time. For determination of the AcCoA kinetic parameters, solutions of AcCoA (0–500 μM, final concentration) were used to initiate reactions containing KAN (500 μM), Eis_*Ban* (0.25 μM), DTNB (2 mM), and Tris (50 mM, pH 8.0). All experiments were performed at least in triplicate. Linear regression was used to obtain reaction velocities for each time course, with negligible uncertainly. These independently measured velocity values were plotted, and Michaelis–Menten parameters were determined without averaging or other data conversion by nonlinear regression with SigmaPlot 12.3 software (SysStat). Kinetic parameters are presented in Table 2, and representative curves can be seen in Figure S5, Supporting Information.

Determination of Positions Acetylated on NEA by Eis_*Ban* by TLC. To visualize which positions of NEA become acetylated by Eis_*Ban*, reactions (40 μL) containing Tris (50 mM, pH 8.0), AcCoA (4 mM, 5 equiv), NEA (0.8 mM, 1 equiv), and Eis_*Ban* (5 μM) were incubated at room temperature, and aliquots were spotted on TLC plates at various times (0, 1, 5, 10, 30 min, and overnight reaction). The mobile phase consisted of 3:0.8/MeOH:NH_4OH. The TLC plates were visualized with a cerium-molybdate stain. The R_f values found for the Eis_*Ban* reactions were in good agreement with those previously reported for Eis_*Mtb*.[27]

Inhibition of Eis_*Ban* by Inhibitors of Eis_*Mtb*. The IC_{50} values for chlorhexidine (**1**) and compounds **2**–**3** (Table 3 and Figure S6, Supporting Information) were determined in a manner similar to that previously reported.[35] Briefly, reactions (200 μL) contained compounds **1**–**3** dissolved in Tris-HCl buffer (50 mM, pH 8.0, 10% DMSO) with a 5-fold serial dilution, Eis_*Ban* enzyme (0.25 μM), and NEO (100 μM), AcCoA (0.5 mM), and DTNB (2 mM). Reagents were added in a stepwise manner, allowing the enzyme to incubate with the inhibitor and NEO, and the reactions were initiated with the AcCoA in solution with DTNB. The reactions were monitored as described for the kinetic analysis. The determination of IC_{50} values was done with a Hill plot analysis using Kaleidagraph 4.1 software.

Table 2. Apparent Steady-State Kinetic Parameters for [AG]-Dependent and [AcCoA]-Dependent Acetylation by Eis from Various Bacteria

(co)substrate	K_m (μM)	k_{cat} (s^{-1})	k_{cat}/K_m (M^{-1} s^{-1})
Eis_*Ban*			
AMK	1070 ± 470	0.10 ± 0.02	92 ± 45
APR	275 ± 80	0.13 ± 0.01	469 ± 140
KAN	57 ± 9	0.135 ± 0.008	2370 ± 400
NEO	469 ± 70	0.186 ± 0.004	397 ± 60
PAR	44 ± 11	0.019 ± 0.001	430 ± 110
SIS	76 ± 31	0.017 ± 0.002	225 ± 95
AcCoA[a]	32 ± 8	0.241 ± 0.014	6700 ± 1700
Eis_*Ava*[b]			
AMK	–[d]	–	–
APR	340 ± 100	0.019 ± 0.002	57 ± 18
KAN	1000 ± 40	0.205 ± 0.004	205 ± 9
NEO	101 ± 16	0.106 ± 0.006	1050 ± 180
PAR	237 ± 36	0.18 ± 0.01	770 ± 130
SIS	–	–	–
Eis_*Msm*[c]			
AMK	251 ± 55	0.034 ± 0.003	13 ± 3
APR	150 ± 43	0.019 ± 0.002	127 ± 39
KAN	655 ± 42	0.36 ± 0.01	541 ± 37
NEO	110 ± 14	0.148 ± 0.006	1345 ± 180
PAR	730 ± 160	0.24 ± 0.03	320 ± 80
SIS	82 ± 8	0.206 ± 0.006	2512 ± 256
AcCoA	39 ± 17	0.40 ± 0.06	10210 ± 4450
Eis_*Mtb*[c]			
AMK	42 ± 9	0.103 ± 0.006	2450 ± 545
APR	×[e]	×	×
KAN	330 ± 40	0.53 ± 0.03	1590 ± 250
NEO	122 ± 23	0.61 ± 0.03	5000 ± 970
PAR	110 ± 21	0.14 ± 0.01	1,240 ± 260
SIS	166 ± 36	1.1 ± 0.1	6810 ± 1,650
AcCoA	10 ± 3	0.094 ± 0.004	9400 ± 2,850

[a]The kinetic parameters for the [AcCoA]-dependent acetylation by Eis_*Ban*, Eis_*Msm*, and Eis_*Mtb* were performed with KAN. [b]These data were previously reported.[26] [c]These data were previously reported.[28] [d]–, indicates this data was not available. [e]×, indicates the AG was not a substrate of the enzyme.

Table 3. IC_{50} Values of Eis_*Mtb* Inhibitors with Various Eis Homologues

	IC_{50} (μM)			
compound	Eis_*Ban*	Eis_*Ava*[a]	Eis_*Msm*[a,b]	Eis_*Mtb*[c]
chlorhexidine (**1**)	14 ± 4	20 ± 7	1.9 ± 0.4	0.19 ± 0.03
2	>200	>200	0.9 ± 0.2	1.09 ± 0.14
3	>200	>200	1.7 ± 0.3	1.24 ± 0.16

[a]These data previously reported.[26] [b]These data previously reported.[26,28] [c]These data previously reported.[35]

DOI: 10.1021/acs.biochem.5b00244
Biochemistry 2015, 54, 3197–3206

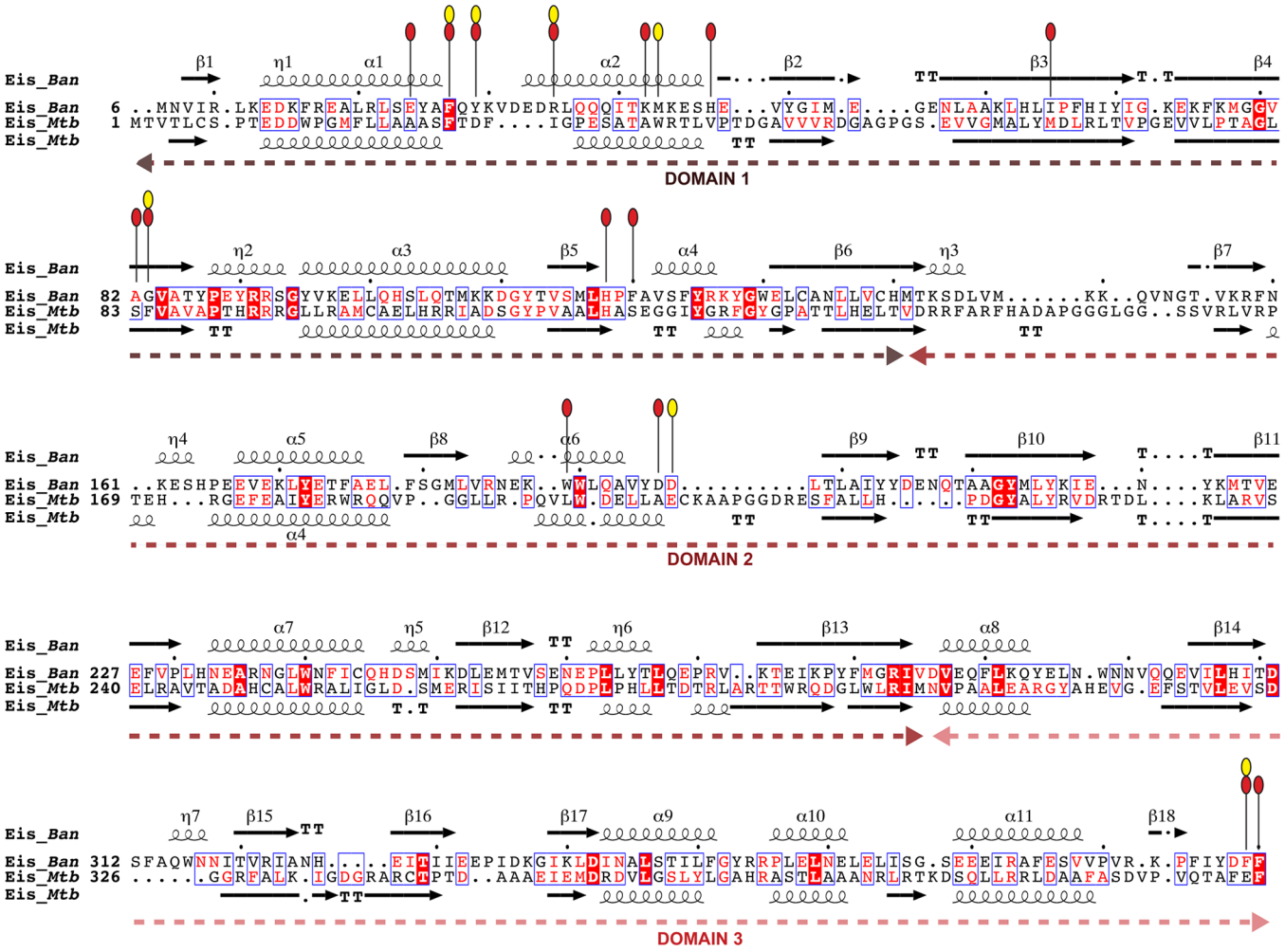

Figure 1. Structure-based protein sequence alignment of Eis proteins from *B. anthracis* (Eis_*Ban*) and from *M. tuberculosis* H37Rv (Eis_*Mtb*). The two Eis homologues exhibit 18% sequence identity. The residues in the immediate active site of Eis_*Mtb* (also shown as sticks in Figure 4B) are marked by red ovals above the alignment and show stark dissimilarities with their counterpart in Eis_*Mtb*. Residues previously identified to bind to TOB in a structure of a TOB-CoA-Eis_*Mtb* structure (PDB ID: 4JD6)[44] are marked by yellow ovals. The residue numbering corresponds to accession code YP_029001.

Crystallization of Eis_*Ban*. Eis_*Ban* at 30 mg/mL was crystallized using sitting drop vapor diffusion at 297 K in a Crystal Quick VR 96-well round-bottomed plate (Greiner Bio-One North America). Eis_*Ban* (400 nL) was mixed with 400 nL of crystallization reagent using a Mosquito VR nanoliter liquid workstation (TTP LabTech) and allowed to equilibrate against 135 μL of crystallization reagent. Four different crystallization screens were used: MCSG-1, MCSG-2, MCSG-3, and MCSG-4 (Microlytic). The best crystals were obtained in the 93th condition of MCSG-1 containing 0.1 M sodium HEPES pH 7.0, 0.2 M sodium chloride, and 20% polyethylene glycol 3350 at 24 °C. The crystals were cryoprotected using the solution prepared by adding 15% (v/v) glycerol to the crystallization condition and flash-frozen in liquid nitrogen. Single wavelength anomalous diffraction data at the selenium peak was collected from the SeMet-substituted protein. The data sets were collected on ADSC quantum Q315r charged coupled device detector at 100 K in the 19ID beamline of the Structural Biology Center at the Advanced Photon Source, Argonne National Laboratory. The crystal belongs to space group $P2_1$ with cell parameters of a = 79.4 Å, b = 176.9 Å, c = 110.0 Å, $\alpha = \gamma = 90°$, $\beta = 105.7°$. The diffraction data were processed by using the HKL3000 suite of programs.[36] Data collection statistics are presented in Table S2, Supporting Information.

Structural Analysis of Eis_*Ban*. All procedures for SAD phasing, phase improvement by density modification, and initial protein model building were performed by the structure module of the HKL3000 software package.[36] The mean figure of merit of the phase set was 0.257 for 50−2.75 Å resolution data and improved to 0.899 after density modification (DM). The script build module using resolve in HKL3000 built 1781 out of 2310 residues, while side chain of 520 residues were placed. The initial model was rebuilt with the program Coot[37] by using electron density maps based on DM-phased reflection file. After each cycle of rebuilding, the model was refined by using REFMAC5 from the CCP4 suite with TLS refinement.[38,39] The geometrical properties of the model were assessed by the Coot and Molprobity software.[40]

Construction of the Δ*eis* Mutant of *B. anthracis* Sterne 34F2. A markerless, in-frame deletion of the *eis* allele that fused the first 10 codons of the gene with the final 10 codons (9 codons plus the native stop codon) was created using PCR. This mutant allele therefore had the internal 1098-bp of the gene removed. The PCR construct also consisted of 521-bp of upstream homology and 514-bp of downstream homology flanking the

DOI: 10.1021/acs.biochem.5b00244
Biochemistry 2015, 54, 3197−3206

deleted gene and was generated by standard overlap extension PCR using the 5′ primer AAGGAAGATAAACGTAAGCC-GTTTATTTATGATTTCT and the 3′ primer AAACG-GCTTACGTTTATCTTCCTTTAATCGTATAACG. This PCR product was cloned into the allelic exchange vector pBKJ236 at the *Not*I and *Bam*HI sites, and allelic exchange was performed as previously described[41] with the following modification: plasmid pSS4332 (a kind gift from Dr. Scott Stibitz, FDA, Division of Bacterial, Parasitic, and Allergenic Products, Center for Biologics Evaluation and Research, Maryland, MD) was used in place of plasmid pBKJ223 to promote the second recombination event needed for allelic exchange. Successful exchange was determined using PCR with primers that anneal to sequences upstream and downstream of the cloned region (5′ primer CGCGCGGCCGCCCTG-TAATTGCATTAGCGGCAACGC; 3′ primer CGCGG-ATCCCTAAACTGTTCACGAATATTTGCGT). The mutant allele yielded a ∼1.1-kb smaller product than the wild-type using this assay. The final mutant contained no added antibiotic resistance and should therefore be isogenic to the wild-type parent.

Determination of MIC and MBC Values for Various Antibiotics against the Δ*eis Ban* Strain. MIC and MBC values were determined against 14 AGs (AMK, G418, GEN, HYG, KAN, NEA, NEO, NET, PAR, RIB, SIS, SPT, STR, and TOB), one β-lactam (ampicillin), two fluoroquinolones (ciprofloxacin and norfloxacin), one polyketide (erythromycin), a compound of nonribosomal peptide origin (chloramphenicol), and the antituberculosis drug isoniazid (Table S3, Supporting Information). Using the microdilution method,[42] MIC values were determined in brain-heart infusion (BHI) broth. The MIC value was determined as the lowest concentration of the inhibitor that did not support bacterial growth, and this determination was confirmed for the respective well by staining with a solution of MTT (50 μL of 1 mg/mL). MBC values were determined by plating all cultures from all wells (20 μL of each) that showed no bacterial growth (prior to staining) on BHI-agar plates. The lowest concentration to show no additional growth after incubation at 37 °C was deemed the MBC value. All MIC and MBC tests were done at least in duplicate.

RESULTS

Comparison of Sequence Features. On the basis of its amino acid sequence, it is clear that Eis_*Ban* and Eis_*Mtb* belong to the same family of the GNAT superfamily of *N*-acyltransferases. However, the amino acid sequence identity is 18% between the Eis_*Ban* and Eis_*Mtb*, and the structure-based sequence alignment indicates that many of the AG binding pocket residues are distinctly different (Figure 1). This prompted us to investigate the substrate selectivity and recognition properties of Eis_*Ban*, both biochemically and structurally.

Substrate Specificity and Multiacetylation Profiles of Eis Proteins. We recently reported the structural and biochemical features of Eis_*Mtb*,[27,30,43−45] as well as biochemical characteristics of its close homologue Eis_*Msm*[28,46] and that of a less homologous protein Eis_*Ava*.[26] These studies revealed that all three enzymes function as aminoglycoside acetyltransferases (AACs) and are capable of multiacetylating AGs. In this work, we performed similar studies to investigate the number of acetylations catalyzed by Eis_*Ban* on a panel of 12 AGs (Table 1). The acetylation results of Eis_*Ban* along with those of other Eis homologues previously determined, for comparison, are presented in Table 1.

We performed an AcCoA titration assay and monitored the reaction products using a UV−vis assay (Figure S3) and mass spectrometry (Figure S4 and Table S1) to show that Eis_*Ban* catalyzed monoacetylation of NET, diacetylation of AMK, APR, HYG, KAN, and SIS, as well as triacetylation of NEA, NEO, PAR, and RIB. In addition, we found that SPT, STR, and TOB were not used as substrates by Eis_*Ban*.

Steady-State Kinetic Analysis of Eis Proteins. In an effort to further highlight and elucidate differences among Eis homologues, we determined Michaelis−Menten kinetic parameters (K_m and k_{cat}) of Eis_*Ban* toward various AGs with AcCoA as the cosubstrate. The kinetic parameters for Eis_*Ban* and that of other previously reported Eis homologues for comparison are presented in Table 2. The apparent K_m value of 32 ± 8 μM for AcCoA determined in the kinetic experiments where its concentration was varied was much smaller than the concentration of AcCoA (500 μM) used in experiments at varying concentrations of AGs. Therefore, the K_m values for different AGs, as with other Eis homologues,[28,43] should be interpreted as the K_m values for AGs interacting with the binary complex of Eis_*Ban*-AcCoA as a reactant. Moreover, given a similar random-sequential mechanism of acetylation with respect to the order of binding of AcCoA and AG,[43] these K_m values correspond to the apparent equilibrium constants for binding of AGs to the Eis_*Ban*-AcCoA complex. Further interpretation of these K_m and k_{cat} values in terms of microscopic mechanistic parameters depends on the number of acetylations per an AG-binding event and may be complicated by potentially different efficiencies of acetylations at different positions for a given AG. On the basis of our recent crystal structure of Eis_*Mtb* in complex with CoA and TOB, after the first acetylation, TOB would likely need to dissociate from the enzyme completely in order to rebind the enzyme for the second major acetylation, as there is not enough space in the binding site for its reorientation without a major protein conformational change. Therefore, acetylation of TOB and, similarly, other AGs would not be processive. If the individual acetylations are carried out with the same efficiency, then the K_m needs to be multiplied by the number of acetylations per AG to obtain the equilibrium constant for binding of an AG to Eis-AcCoA complex, and k_{cat} represents the true catalytic efficiency for an individual acetylation event. In the other extreme, when the mechanism is fully processive, i.e., an AG gets fully acetylated upon binding to the enzyme once, the K_m values reported in Table 2 are interpreted as true equilibrium constants for binding of an AG to Eis-AcCoA compex, whereas the k_{cat} is a rate constant averaged over all acetylation events for this AG.

TLC-Based Analysis of Positions of Acetylation on NEA by Eis_*Ban*. We previously demonstrated that both Eis_*Mtb*[27] and Eis_*Msm*[28] sequentially acetylate NEA at the 2′-, 6′-, and 1-positions. To test whether Eis_*Ban* also sequentially acetylates NEA at these positions, we performed TLC analysis of the reaction of AcCoA with NEA in the presence of Eis_*Ban* over a period of 24 h (Figure 2). The production of 2′,6′-diacetyl-NEA was observed after 1 min as determined by comparing the R_f of this compound to that of the previously reported reaction for Eis_*Mtb* under identical conditions. After 5 min, a product appeared whose R_f is congruent with that of 2′,6′,1-triacetyl-NEA. All NEA was consumed after a 30 min of incubation, and only a mixture of spots with similar retention factor (R_f) values to those of 2′,6′-diacetyl-NEA and 2′,6′,1-triacetyl-NEA, as generated by Eis_*Mtb*,[27] was observed. The reaction was incubated for an additional 16−20 h and a mixture of both

DOI: 10.1021/acs.biochem.5b00244
Biochemistry 2015, 54, 3197−3206

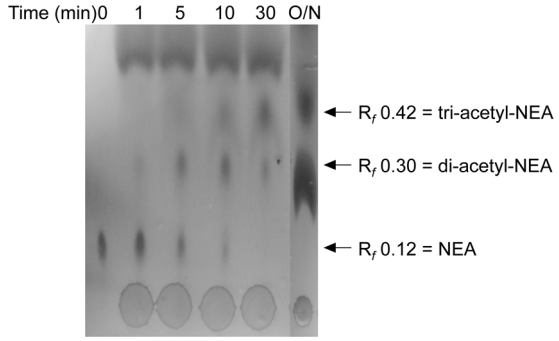

Figure 2. Multiacetylation by Eis_*Ban* of NEA over time (0, 1, 5, 10, and 30 min and overnight reactions) observed in TLC assay. The R_f values of 0.12, 0.30, and 0.42 represent NEA, 2′,6′-diacetyl-NEA, and 2′,6′,1-triacetyl-NEA, respectively (as these R_f values match those previously reported for these NEA derivatives generated by Eis_*Mtb*).[27]

triacetylated- and diacetylated-NEA remained. These data indicate that the 2′- and the 6′-acetylation events, whose order is unclear, are followed by the 1-acetylation of NEA by Eis_*Ban*.

Inhibition of Eis Proteins. To further probe the differences in the active sites of Eis_*Ban* and other Eis homologues, we investigated inhibitory properties of three inhibitors of Eis_*Mtb*, chlorhexidine (**1**) and compounds **2** and **3**, which we recently identified from a high-throughput screening study with Eis_*Mtb* (Figure S1C and Table 3).[35] Of the compounds tested, which were all good inhibitors of both Eis_*Mtb* and Eis_*Msm*, just as in the case of Eis_*Ava*, only chlorhexidine showed detectable inhibition of Eis_*Ban* with an IC_{50} value of 14 ± 4 μM (Table 3 and Figure S6).

Overall Structure of Eis_*Ban*. In order to understand the interactions that dictate recognition and acetylation of AGs by Eis_*Ban*, we crystallized and determined a crystal structure of Eis_*Ban* (Figure 3). The crystals diffracted to 2.75 Å resolution and belonged to space group $P2_1$ with one hexamer in the asymmetric unit. The experimental data collection and refinement statistics are given in Table S2. A superposition of this structure with that of Eis_*Mtb* (PDB ID: 3R1K[27]) showed that the monomers superpose well and display similar hexameric assemblies (Figure 4A).

Active Site Structure of Eis_*Ban*. The entire electron density map including that of the active site area was reasonably ordered for all six polypeptide chains in the asymmetric unit. As in other Eis homologues, each subunit of the 385-residue Eis_*Ban* contains three domains. The residue directly involved in the catalytic acetyl group transfer chemistry and proposed to be a general acid in the *Mtb* homologue, Tyr125, and the C-terminal residue as well as the location of the carboxyl terminal group of the protein, the last proposed to serve a general base, are conserved (Figure 1). The exact CoA position can also be predicted with high certainty due to the conserved nature of this cosubstrate-binding site and comparison to other CoA-bound structures of other Eis homologues. However, the backbones of the loops bearing residues lining the active site adopt considerably different conformations (Figures 1 and 4B). A close look at the active site indicates that the putative AG binding residues are also highly dissimilar (Figures 1 and 4B). Out of approximately 15 residues forming the substrate-binding site, only 3 residues are the same, 6 residues are similar, and 6 residues are very different. As a result, the shape and the surface-charge properties of the active site pocket of Eis_*Ban* are significantly different from those of Eis_*Mtb* (Figure 5). Overall, the substrate-binding pocket of Eis_*Ban* appears more open, and the face of the pocket formed by the N-terminal domain (Figure 5A,D) is less negatively charged than in Eis_*Mtb* (Figure 5B,E).

MIC and MBC Studies of Antibiotics against the Δ*eis Ban* Strain. To investigate if Eis_*Ban* affects the antibacterial susceptibility of *B. anthracis*, we generated a mutant strain of *B. anthracis* 34F2 Sterne in which the *eis* gene was deleted (Δ*eis Ban*). We determined MIC and MBC values for 20 antibiotics

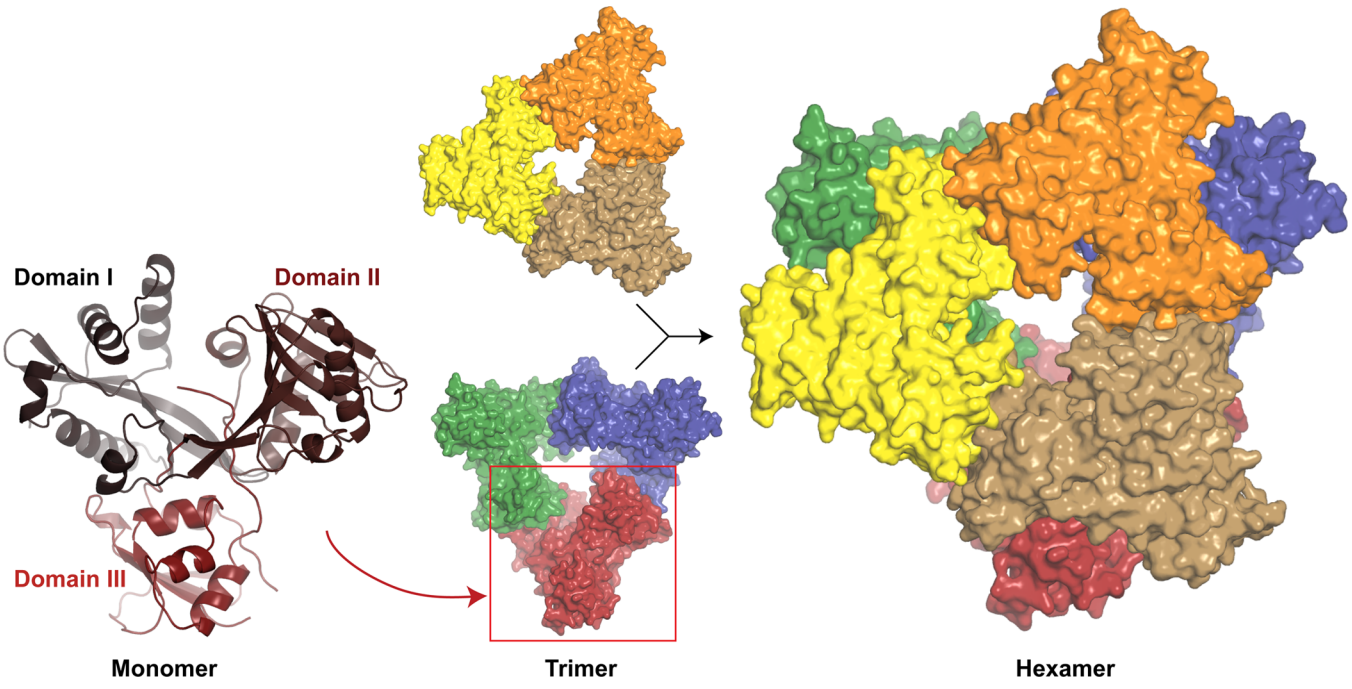

Figure 3. Structure of Eis_*Ban*. Left: A cartoon representation of the Eis_*Ban* monomer. The three domains are highlighted in different shades of red. Middle: surface representation of its trimeric and Right: hexameric assembly forms, with each monomer highlighted in a different color.

DOI: 10.1021/acs.biochem.5b00244
Biochemistry 2015, 54, 3197−3206

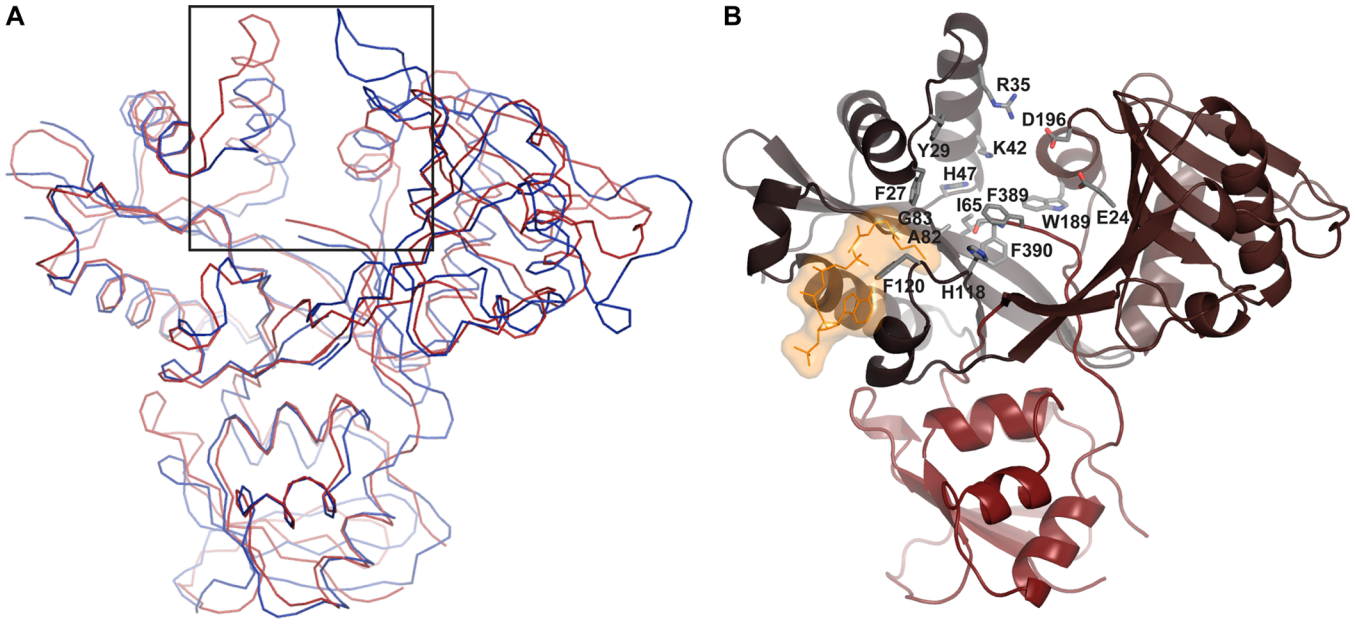

Figure 4. (A) The superposition of Eis_*Ban* (brown) and Eis_*Mtb* (dark blue) showing overall structural similarity but drastic changes in loops around the active site (indicated with the black square). (B) A close-up cartoon representation view of the monomer of Eis_*Ban* with residues in its immediate active site pocket marked (Note: these residues are marked by red ovals in Figure 1). The CoA binding site is shown in orange.

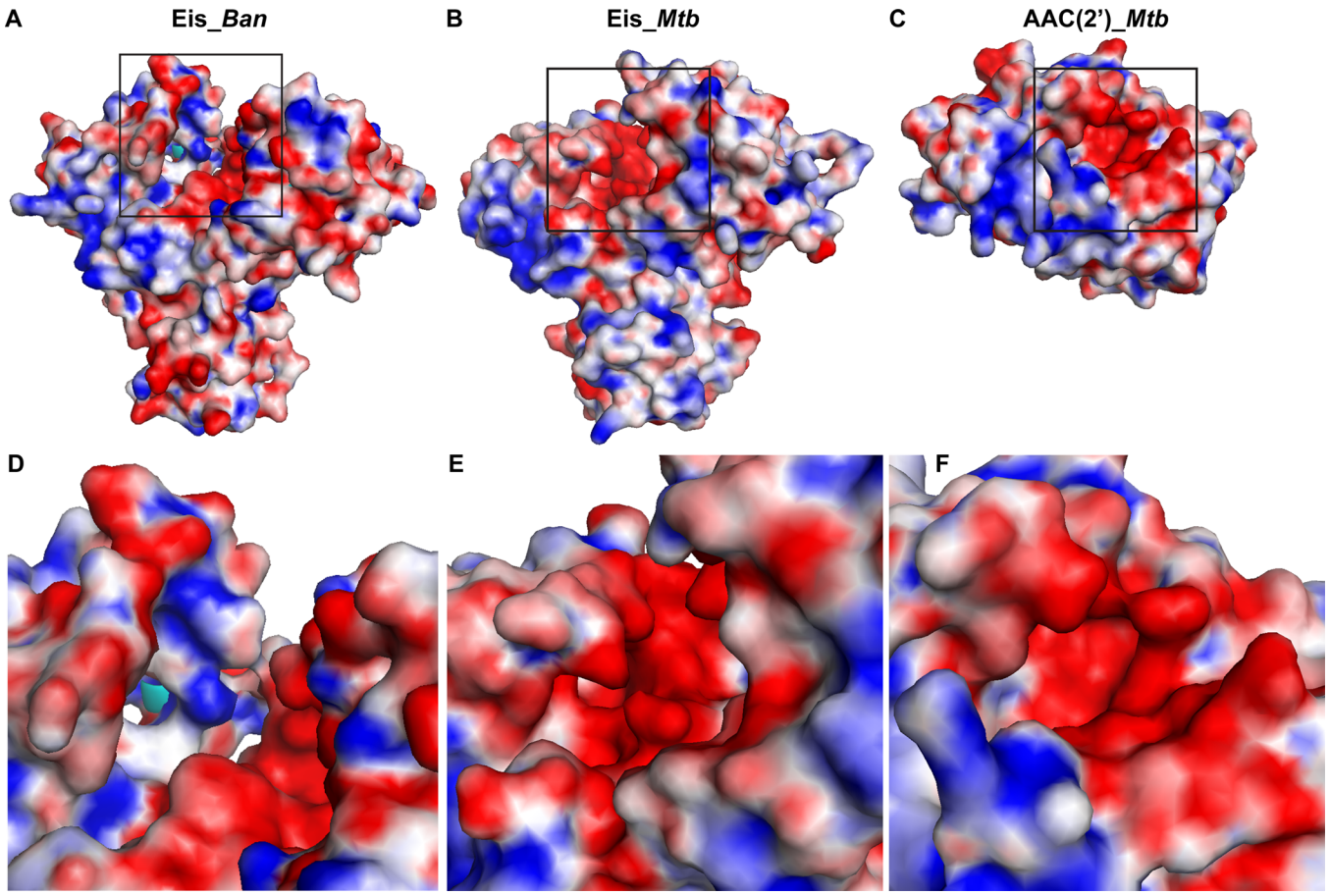

Figure 5. Surface electrostatics of (A) Eis_*Ban*, (B) Eis_*Mtb*, and (C) AAC(2′)-Ic from *M. tuberculosis*; D, E, and F are magnified views of the immediate active site highlighting stark differences.

against wild-type and Δ*eis Ban* (Table S3). The deletion strain did not have an apparent growth defect, indicating that the *eis* gene is not essential for growth of *B. anthracis* in rich media. Furthermore, MIC values for all AG and non-AG antibiotics were the same for the wild-type and Δ*eis Ban* within a 2-fold dilution,

DOI: 10.1021/acs.biochem.5b00244
Biochemistry 2015, 54, 3197−3206

indicating that basal levels of Eis_*Ban* do not contribute to antibiotic resistance.

DISCUSSION

The natural and engineered strains of *B. anthracis* pose a potential threat of rapid infection and global spread. Efforts to treat anthrax infections have primarily focused on developing effective vaccines. However, in the event a human or livestock becomes infected, effective antimicrobial agents will be necessary, and this raises an urgent call for effective antibiotics. GEN is a potent AG antibiotic that is used in combination therapy for inhalation anthrax disease.[47] Other AG antibiotics such as NEO and STR have also proven to be effective against *B. anthracis*,[20] and synthetic AGs have been shown to act as potent inhibitors of anthrax lethal factor.[20,25] To develop suitable AG antibiotics against presently found *B. anthracis* strains, we require a clear understanding of the resistance factors naturally present in these bacteria. Here, we focus on a highly potent and versatile acetyltransferase, Eis_*Ban*. We demonstrate here that Eis_*Ban*, similarly to its *M. tuberculosis* homologue, is neither essential for bacterial growth on rich media nor contributes to antibiotic resistance when expressed at basal levels. However, upregulation of Eis_*Ban* may cause resistance against chemotherapeutic agents of the AG class, as observed in mycobacteria.[31] As in *M. tuberculosis*, *Ban* strains with upregulated Eis_*Ban* expression may arise through selective pressure of AG administration, as a result of promoter mutations. The biological need of acetylation function of Eis is still unclear. Little is known about the involvement of Eis in cellular metabolic pathways or its role in host invasion and infection, if any. Recent studies indicate that lysine or arginine residues of other proteins such as DUSP16/MKP7 are substrates of the Eis_*Mtb* homologue and Eis_*Mtb* might be involved in *N*-acetyltransferase activity against a plethora of other peptide substrates.[29] Nonetheless, this enzyme possesses a particularly unusual multiacetylating capability against AGs. Here, we investigated the structure−function relationship of Eis_*Ban* to gain a better understanding of its acetyltransferase specificity and to elucidate what type of AG modification would be significant, should resistance due to Eis_*Ban* arise. In addition, understanding of the specificity determinants in the active site could enable us to rationally modify AGs and generate new potential AG drugs against Eis_*Ban* or other pathogenic bacteria.

Resistance enzymes AG acetyltransferases (AACs) found in many pathogenic bacteria are known to monoacetylate the amine moiety at the 6′-, 2′-, or 3-position of various AGs. These regiospecific AACs are characterized by a negatively charged AG binding pocket formed in a single GNAT domain (Figure 5C). The small size of the binding pocket of these AACs likely dictates a unique orientation of a bound AG, in turn defining its regiospecificity. In contrast, the Eis family of proteins exhibits unusual regioversatility as acetyltransferases, modifying many AGs at multiple positions. This multiacetylation is enabled by a significantly larger negatively charged AG binding pocket formed by two conjoined GNAT domains.[27,44] Because the ability to acetylate a given AG and the regioversatility will primarily depend on the shape and the properties of residues in AG binding site of an Eis homologue,[26−28] we explored the biochemical properties and structural features of Eis_*Ban*.

For the panel of examined AGs, the Eis_*Ban* modifies the same number or fewer amines than does the Eis_*Mtb* homologue for all but two AGs, APR and PAR (Table 1). This lesser regioversatility is likely due to the somewhat less negatively charged AG binding pocket of Eis_*Ban*. APR, which is not acetylated by Eis_*Mtb*, is diacetylated by Eis_*Ban*. The ability to acetylate a relatively stiff APR molecule by Eis was previously shown to be dictated by the size of the AG binding pocket and to be specifically sensitive to the nature of the residue in place of Trp289 of Eis_*Mtb*.[46] The residue found in place of this Trp residue in Eis_*Ban* is a more flexible Glu275 (Figure 1); in addition, the backbone bearing this residue is shifted resulting in the more open pocket. We propose that this more open and malleable substrate binding pocket feature is what allows APR to be accommodated and acetylated by Eis_*Ban*. We speculate that the hydroxyl group of PAR at the 6′-position allows this AG to bind the active site pocket of Eis_*Ban* in an orientation that is disfavored in the more negatively charged pocket of Eis_*Mtb*, thus leading to an additional acetylation by Eis_*Ban*. Strikingly, TOB is not a substrate for Eis_*Ban*, while Eis_*Mtb* can acetylate TOB at up to four positions (Table 1).[27,44] Residues Asp26 and Glu401 of Eis_*Mtb* were recently demonstrated to interact directly with amino groups of the bound TOB in a crystal structure of Eis_*Mtb*-TOB complex.[44] In contrast, Eis_*Ban* contains Tyr29 and Phe389 in structurally analogous positions (Figure 1). The inability of these residues to form salt bridges with TOB amines likely prevents TOB from binding properly for its acetylation by Eis_*Ban*.

Of the tested inhibitors of Eis_*Mtb* only one displayed any activity with Eis_*Ban*, chlorhexidine (**1**). This inhibitor showed a 77-fold preference for Eis_*Mtb* (IC_{50} = 0.188 μM) over Eis_*Ban* (IC_{50} = 14 μM) further stressing the global differences in the charge and shape of the AG binding pockets of these enzymes.

While it is known that upregulation of Eis_*Mtb* causes resistance of *Mtb* to KAN, Eis_*Mtb* is not essential for bacterial growth *in vitro*.[31] In order to better understand the physiological role of Eis protein in *Ban*, we decided to delete the *eis* gene from the bacterial genome and compare how the wild-type (*B. anthracis* 34F2 Sterne strain) and the mutant reacted to AG treatment. We successfully removed the gene encoding Eis from the *B. anthracis* genome using a markerless gene replacement protocol.[41] This is corroborated by the MIC data (Table S3). All MIC values for the wild-type *Ban* and the Δ*eis Ban* differ by no more than 2-fold. The MIC data indicate that, currently, the presence of Eis, in *Ban*, does not contribute to resistance to AGs. *Mtb* only becomes resistant to KAN and AMK through the upregulation of Eis_*Mtb* due to a mutation in its promoter region. Therefore, it is not surprising that wild-type *Ban* and Δ*eis Ban* have similar MIC values. A difference between the two phenotypes was more apparent when we compared the bactericidal and bacteriostatic properties of the antibiotic compounds. With the exception of isoniazid, all compounds were bacteriostatic at or near the MIC concentration. While for most antibiotic compounds there was no difference between the MBC for the wild-type and Δ*eis Ban* there are a few noteworthy exceptions. HYG was observed to be bactericidal with the wild-type *Ban*, but when tested with the Δ*eis Ban* was bacteriostatic up to the highest concentration tested (188 μg/mL). This is the opposite of what we expected and may point to a distinct function of the enzyme *in vivo*. NEA was bactericidal for both phenotypes of *Ban*; however, the bactericidal dose of wild-type *Ban* was four times higher than that for the Δ*eis Ban*.

In conclusion, we showed the Eis_*Ban* is a unique member of the Eis family with the ability to acetylate a variety of AGs generally at multiple positions. The unique range of multi-acetylation of the AGs exhibited by Eis_*Ban* must be a result of its divergently evolved AG binding pocket. Future research

DOI: 10.1021/acs.biochem.5b00244
Biochemistry 2015, 54, 3197−3206

unveiling the *in vivo* function of Eis might shed light on these recognition signatures. Consistent with these observations are differences in kinetics parameters for AG acetylation, and the lack or significantly reduced inhibition of Eis_*Ban* by Eis_*Mtb*. This characterization improves our understanding of AG recognition by Eis and allows one to foresee the potential of *B. anthracis* to acquire resistance toward specific AGs upon Eis upregulation to optimize therapeutic regimens.

■ ASSOCIATED CONTENT

Supporting Information

Figure S1. Chemical structures of G substrates, other antibiotics, and Eis_*Mtb* inhibitors tested against Eis_*Ban*. Figure S2. Coomassie blue-stained 15% Tris-HCl SDS-PAGE gel showing 6 μg of Eis_*Ban*. Figure S3. Representative examples of spectrophotometric assay plots showing the conversion of a variety of AGs by Eis_*Ban* to their di- and tri-acetylated counterparts. Figure S4. Mass spectra of AGs multi-acetylated by Eis_*Ban*. Table S1. Mass analysis of AGs acetylated by Eis_*Ban*. Figure S5. Michaelis-Menten analysis of the Eis_*Ban* catalyzed acetylation of selected AGs. Figure S6. Hill plot of inhibition of Eis_*Ban* by chlorhexidine (**1**). Table S2. X-ray diffraction data collection and refinement statistics for the Eis_*Ban* structure. Table S3. MIC and MBC values of antibiotics against wild-type *Ban* and Δ*eis Ban*. The Supporting Information is available free of charge on the ACS Publications website at DOI: 10.1021/acs.biochem.5b00244.

■ AUTHOR INFORMATION

Corresponding Author

*E-mail: sylviegtsodikova@uky.edu; phone: 859-218-1686; fax: 859-257-7585.

Author Contributions

◆K.D.G. and T.B. contributed equally to this work.

Funding

This work was supported by the National Institute of Health (NIH) Grants AI090048 (to S.G.-T.), GM074942 (to A.J.), GM094585 (to A.J.), and by startup funds from the College of Pharmacy at the University of Kentucky (to S.G.-T. and O.V.T.). The use of SBC 19ID was supported by the U.S. Department of Energy, Office of Biological and Environmental Research, under contract DE-AC02−06CH11357.

Notes

The authors declare no competing financial interest.

■ ACKNOWLEDGMENTS

The authors wish to thank members of the Structural Biology Center, especially Dr. Rongguang Zhang, at Argonne National Laboratory, for their help with data collection at the 19ID beamline.

■ ABBREVIATIONS

AcCoA, acetyl-coenzyme A; AMK, amikacin; AG, aminoglycoside; AAC, aminoglycoside acetyltransferase; APH, aminoglycoside phosphotransferase; APR, apramycin; *Ava*, *Anabaena variabilis*; *Ban*, *Bacillus anthracis*; DTNB, 5,5′-dithiobis(2-nitrobenzoic acid); Eis, enhanced intracellular survival; equiv, equivalent; G418, geneticin; GEN, gentamicin; HYG, hygromycin; KAN, kanamycin A; LCMS, liquid chromatography mass spectrometry; MBC, minumum bactericidal concentration; MIC, minumum inhibitory concentration; *Msm*, *Mycobacterium smegmatis*; *Mtb*, *Mycobacterium tuberculosis*; NEA, neamine; NEO, neomycin B; NET, netilmicin; PAR, paromomycin; RIB, ribostamycin; SIS, sisomicin; SPT, spectinomycin; STR, streptomycin; TLC, thin-layer chromatography; TOB, tobramycin; TB, tuberculosis

■ REFERENCES

(1) Bottone, E. J. (2010) *Clin. Microbiol. Rev. 23*, 382−398.

(2) Holty, J. E., Bravata, D. M., Liu, H., Olshen, R. A., McDonald, K. M., and Owens, D. K. (2006) Systematic review: a century of inhalational anthrax cases from 1900 to 2005. *Ann. Int. Med. 144*, 270−280.

(3) Brookmeyer, R., Johnson, E., and Bollinger, R. (2004) Public health vaccination policies for containing an anthrax outbreak. *Nature 432*, 901−904.

(4) Bouzianas, D. G. (2009) Medical countermeasures to protect humans from anthrax bioterrorism. *Trends Microbiol. 17*, 522−528.

(5) Tierney, B. C., Martin, S. W., Franzke, L. H., Marano, N., Reissman, D. B., Louchart, R. D., Goff, J. A., Rosenstein, N. E., Sever, J. L., and McNeil, M. M. (2003) Serious adverse events among participants in the Centers for Disease Control and Prevention's Anthrax Vaccine and Antimicrobial Availability Program for persons at risk for bioterrorism-related inhalational anthrax. *Clin. Infect. Dis. 37*, 905−911.

(6) Wright, J. G., Quinn, C. P., Shadomy, S., and Messonnier, N. (2010) Use of anthrax vaccine in the United States: recommendations of the Advisory Committee on Immunization Practices (ACIP), 2009. *MMWR Recommendations Rep. 59*, 1−30.

(7) Burnett, J. C., Henchal, E. A., Schmaljohn, A. L., and Bavari, S. (2005) The evolving field of biodefence: therapeutic developments and diagnostics. *Nat. Rev. Drug Discovery 4*, 281−297.

(8) Loveless, B. M., Yermakova, A., Christensen, D. R., Kondig, J. P., Heine, H. S., 3rd, Wasieloski, L. P., and Kulesh, D. A. (2010) Identification of ciprofloxacin resistance by SimpleProbe, high tesolution melt and pyrosequencing nucleic acid analysis in biothreat agents: *Bacillus anthracis*, *Yersinia pestis* and *Francisella tularensis*. *Mol. Cell Probes 24*, 154−160.

(9) Brouillard, J. E., Terriff, C. M., Tofan, A., and Garrison, M. W. (2006) Antibiotic selection and resistance issues with fluoroquinolones and doxycycline against bioterrorism agents. *Pharmacotherapy 26*, 3−14.

(10) Antwerpen, M. H., Schellhase, M., Ehrentreich-Forster, E., Bier, F., Witte, W., and Nubel, U. (2007) DNA microarray for detection of antibiotic resistance determinants in *Bacillus anthracis* and closely related Bacillus cereus. *Mol. Cell Probes 21*, 152−160.

(11) Agren, J., Finn, M., Bengtsson, B., and Segerman, B. (2014) Microevolution during an Anthrax outbreak leading to clonal heterogeneity and penicillin resistance. *PloS One 9*, e89112.

(12) Akoachere, M., Squires, R. C., Nour, A. M., Angelov, L., Brojatsch, J., and Abel-Santos, E. (2007) Identification of an *in vivo* inhibitor of *Bacillus anthracis* spore germination. *J. Biol. Chem. 282*, 12112−12118.

(13) Klimecka, M. M., Chruszcz, M., Font, J., Skarina, T., Shumilin, I., Onopryienko, O., Porebski, P. J., Cymborowski, M., Zimmerman, M. D., Hasseman, J., Glomski, I. J., Lebioda, L., Savchenko, A., Edwards, A., and Minor, W. (2011) Structural analysis of a putative aminoglycoside *N*-acetyltransferase from *Bacillus anthracis*. *J. Mol. Biol. 410*, 411−423.

(14) Beierlein, J. M., Frey, K. M., Bolstad, D. B., Pelphrey, P. M., Joska, T. M., Smith, A. E., Priestley, N. D., Wright, D. L., and Anderson, A. C. (2008) Synthetic and crystallographic studies of a new inhibitor series targeting *Bacillus anthracis* dihydrofolate reductase. *J. Med. Chem. 51*, 7532−7540.

(15) Pfleger, B. F., Lee, J. Y., Somu, R. V., Aldrich, C. C., Hanna, P. C., and Sherman, D. H. (2007) Characterization and analysis of early enzymes for petrobactin biosynthesis in *Bacillus anthracis*. *Biochemistry 46*, 4147−4157.

(16) Biswas, T., Green, K. D., Garneau-Tsodikova, S., and Tsodikov, O. V. (2013) Discovery of inhibitors of *Bacillus anthracis* primase DnaG. *Biochemistry 52*, 6905−6910.

(17) Wu, R., Richter, S., Zhang, R. G., Anderson, V. J., Missiakas, D., and Joachimiak, A. (2009) Crystal structure of *Bacillus anthracis* transpeptidase enzyme CapD. *J. Biol. Chem. 284*, 24406−24414.

DOI: 10.1021/acs.biochem.5b00244
Biochemistry 2015, 54, 3197−3206

(18) Makowska-Grzyska, M., Kim, Y., Maltseva, N., Osipiuk, J., Gu, M., Zhang, M., Mandapati, K., Gollapalli, D. R., Gorla, S. K., Hedstrom, L., and Joachimiak, A. (2015) A Novel cofactor-binding Mode in bacterial IMP dehydrogenases explains inhibitor selectivity. *J. Biol. Chem. 290*, 5893−5911.
(19) Karginov, V. A., Nestorovich, E. M., Moayeri, M., Leppla, S. H., and Bezrukov, S. M. (2005) Blocking anthrax lethal toxin at the protective antigen channel by using structure-inspired drug design. *Proc. Natl. Acad. Sci. U. S. A. 102*, 15075−15080.
(20) Lee, L. V., Bower, K. E., Liang, F. S., Shi, J., Wu, D., Sucheck, S. J., Vogt, P. K., and Wong, C. H. (2004) Inhibition of the proteolytic activity of anthrax lethal factor by aminoglycosides. *J. Am. Chem. Soc. 126*, 4774−4775.
(21) Zawadzka, A. M., Kim, Y., Maltseva, N., Nichiporuk, R., Fan, Y., Joachimiak, A., and Raymond, K. N. (2009) Characterization of a *Bacillus subtilis* transporter for petrobactin, an anthrax stealth siderophore. *Proc. Natl. Acad. Sci. U. S. A. 106*, 21854−21859.
(22) Hammerstrom, T. G., Horton, L. B., Swick, M. C., Joachimiak, A., Osipiuk, J., and Koehler, T. M. (2015) Crystal structure of Bacillus anthracis virulence regulator AtxA and effects of phosphorylated histidines on multimerization and activity. *Mol. Microbiol. 95*, 426−441.
(23) Jiao, G. S., Simo, O., Nagata, M., O'Malley, S., Hemscheidt, T., Cregar, L., Millis, S. Z., Goldman, M. E., and Tang, C. (2006) Selectively guanidinylated derivatives of neamine. Syntheses and inhibition of anthrax lethal factor protease. *Bioorg. Med. Chem. Lett. 16*, 5183−5189.
(24) Kuzmic, P., Cregar, L., Millis, S. Z., and Goldman, M. (2006) Mixed-type noncompetitive inhibition of anthrax lethal factor protease by aminoglycosides. *FEBS J. 273*, 3054−3062.
(25) Fridman, M., Belakhov, V., Lee, L. V., Liang, F. S., Wong, C. H., and Baasov, T. (2005) Dual effect of synthetic aminoglycosides: antibacterial activity against Bacillus anthracis and inhibition of anthrax lethal factor. *Angew. Chem. 44*, 447−452.
(26) Pricer, R. E., Houghton, J. L., Green, K. D., Mayhoub, A. S., and Garneau-Tsodikova, S. (2012) Biochemical and structural analysis of aminoglycoside acetyltransferase Eis from *Anabaena variabilis*. *Mol. Biosyst. 8*, 3305−3313.
(27) Chen, W., Biswas, T., Porter, V. R., Tsodikov, O. V., and Garneau-Tsodikova, S. (2011) Unusual regioversatility of acetyltransferase Eis, a cause of drug resistance in XDR-TB. *Proc. Natl. Acad. Sci. U. S. A. 108*, 9804−9808.
(28) Chen, W., Green, K. D., Tsodikov, O. V., and Garneau-Tsodikova, S. (2012) Aminoglycoside multiacetylating activity of the enhanced intracellular survival protein from *Mycobacterium smegmatis* and its inhibition. *Biochemistry 51*, 4959−4967.
(29) Kim, K. H., An, D. R., Song, J., Yoon, J. Y., Kim, H. S., Yoon, H. J., Im, H. N., Kim, J., Kim do, J., Lee, S. J., Lee, H. M., Kim, H. J., Jo, E. K., Lee, J. Y., and Suh, S. W. (2012) *Mycobacterium tuberculosis* Eis protein initiates suppression of host immune responses by acetylation of DUSP16/MKP-7. *Proc. Natl. Acad. Sci. U. S. A. 109*, 7729−7734.
(30) Houghton, J. L., Green, K. D., Pricer, R. E., Mayhoub, A. S., and Garneau-Tsodikova, S. (2013) Unexpected *N*-acetylation of capreomycin by mycobacterial Eis enzymes. *J. Antimicrob. Chemother. 68*, 800−805.
(31) Zaunbrecher, M. A., Sikes, R. D., Jr., Metchock, B., Shinnick, T. M., and Posey, J. E. (2009) Overexpression of the chromosomally encoded aminoglycoside acetyltransferase eis confers kanamycin resistance in *Mycobacterium tuberculosis*. *Proc. Natl. Acad. Sci. U. S. A. 106*, 20004−20009.
(32) Stols, L., Gu, M., Dieckman, L., Raffen, R., Collart, F. R., and Donnelly, M. I. (2002) A new vector for high-throughput, ligation-independent cloning encoding a tobacco etch virus protease cleavage site. *Protein Express Purif. 25*, 8−15.
(33) Kim, Y., Dementieva, I., Zhou, M., Wu, R., Lezondra, L., Quartey, P., Joachimiak, G., Korolev, O., Li, H., and Joachimiak, A. (2004) Automation of protein purification for structural genomics. *J. Struct. Funct. Genomics 5*, 111−118.
(34) Kim, Y., Babnigg, G., Jedrzejczak, R., Eschenfeldt, W. H., Li, H., Maltseva, N., Hatzos-Skintges, C., Gu, M., Makowska-Grzyska, M., Wu, R., An, H., Chhor, G., and Joachimiak, A. (2011) High-throughput protein purification and quality assessment for crystallization. *Methods 55*, 12−28.
(35) Green, K. D., Chen, W., and Garneau-Tsodikova, S. (2012) Identification and characterization of inhibitors of the aminoglycoside resistance acetyltransferase Eis from *Mycobacterium tuberculosis*. *ChemMedChem 7*, 73−77.
(36) Minor, W., Cymborowski, M., Otwinowski, Z., and Chruszcz, M. (2006) HKL-3000: the integration of data reduction and structure solution–from diffraction images to an initial model in minutes. *Acta Crystallog., Sect. D 62*, 859−866.
(37) Emsley, P., and Cowtan, K. (2004) Coot: model-building tools for molecular graphics. *Acta Crystallogr., Sect. D 60*, 2126−2132.
(38) Sankaran, K., and Wu, H. C. (1994) Lipid modification of bacterial prolipoprotein. Transfer of diacylglyceryl moiety from phosphatidylglycerol. *J. Biol. Chem. 269*, 19701−19706.
(39) Winn, M. D., Murshudov, G. N., and Papiz, M. Z. (2003) Macromolecular TLS refinement in REFMAC at moderate resolutions. *Methods Enzymol. 374*, 300−321.
(40) Davis, I. W., Leaver-Fay, A., Chen, V. B., Block, J. N., Kapral, G. J., Wang, X., Murray, L. W., Arendall, W. B., 3rd, Snoeyink, J., Richardson, J. S., and Richardson, D. C. (2007) MolProbity: all-atom contacts and structure validation for proteins and nucleic acids. *Nucleic Acids Res. 35*, W375−383.
(41) Janes, B. K., and Stibitz, S. (2006) Routine markerless gene replacement in *Bacillus anthracis*. *Infect. Immun. 74*, 1949−1953.
(42) Shaul, P., Green, K. D., Rutenberg, R., Kramer, M., Berkov-Zrihen, Y., Breiner-Goldstein, E., Garneau-Tsodikova, S., and Fridman, M. (2011) Assessment of 6′- and 6‴-N-acylation of aminoglycosides as a strategy to overcome bacterial resistance. *Org. Biomol. Chem. 9*, 4057−4063.
(43) Tsodikov, O. V., Green, K. D., and Garneau-Tsodikova, S. (2014) A random sequential mechanism of aminoglycoside acetylation by *Mycobacterium tuberculosis* Eis protein. *PloS One 9*, e92370.
(44) Houghton, J. L., Biswas, T., Chen, W., Tsodikov, O. V., and Garneau-Tsodikova, S. (2013) Chemical and structural insights into the regioversatility of the aminoglycoside acetyltransferase Eis. *ChemBioChem 14*, 2127−2135.
(45) Chen, W., Green, K. D., and Garneau-Tsodikova, S. (2012) Cosubstrate tolerance of the aminoglycoside resistance enzyme Eis from *Mycobacterium tuberculosis*. *Antimicrob. Agents Chemother. 56*, 5831−5838.
(46) Jennings, B. C., Labby, K. J., Green, K. D., and Garneau-Tsodikova, S. (2013) Redesign of substrate specificity and identification of the aminoglycoside binding residues of Eis from *Mycobacterium tuberculosis*. *Biochemistry 52*, 5125−5132.
(47) Vaiana, A. C., and Sanbonmatsu, K. Y. (2009) Stochastic gating and drug-ribosome interactions. *J. Mol. Biol. 386*, 648−661.

DOI: 10.1021/acs.biochem.5b00244
Biochemistry 2015, 54, 3197−3206